Co-existence of periodic bursts and death of cycles in a population dynamics system

Sudharsana V. Iyengar, Janaki Balakrishnan, and Jürgen Kurths

Citation: Chaos **26**, 093111 (2016); doi: 10.1063/1.4962633
View online: http://dx.doi.org/10.1063/1.4962633
View Table of Contents: http://scitation.aip.org/content/aip/journal/chaos/26/9?ver=pdfcov
Published by the AIP Publishing

Co-existence of periodic bursts and death of cycles in a population dynamics system

Sudharsana V. Iyengar,[1] Janaki Balakrishnan,[2,a)] and Jürgen Kurths[3]
[1]School of Physics, University of Hyderabad, Central University P.O., Gachi Bowli, Hyderabad 500046, India
[2]School of Natural Sciences and Engineering, National Institute of Advanced Studies (N.I.A.S.), Indian Institute of Science Campus, Bangalore 560012, India
[3]Potsdam Institute for Climate Impact Research, PO Box 601203, Potsdam 14412, Germany

(Received 18 May 2016; accepted 26 August 2016; published online 21 September 2016)

We study the dynamics of a discrete-time tritrophic model which mimics the observed periodicity in the population cycles of the larch budmoth insect which causes widespread defoliation of larch forests at high altitudes periodically. Our model employs q-deformation of numbers to model the system comprising the budmoth, one or more parasitoid species, and larch trees. Incorporating climate parameters, we introduce additional parasitoid species and show that their introduction increases the periodicity of the budmoth cycles as observed experimentally. The presence of these additional species also produces other interesting dynamical effects such as periodic bursting and oscillation quenching via oscillation death, amplitude death, and partial oscillation death which are also seen in nature. We suggest that introducing additional parasitoid species provides an alternative explanation for the collapse of the nine year budmoth outbreak cycles observed in the Swiss Alps after 1981. A detailed exploration of the parameter space of the system is performed with movies of bifurcation diagrams which enable variation of two parameters at a time. Limit cycles emerge through a Neimark–Sacker bifurcation with respect to all parameters in all the five and higher dimensional models we have studied. *Published by AIP Publishing.*
[http://dx.doi.org/10.1063/1.4962633]

Large scale, massive defoliation of larch forests at high altitudes due to infestation by the larch budmoth (LBM) insect has been occurring periodically for centuries in different parts of the world. This ecological phenomenon involves three trophic levels: the larch trees represented by their needle length, the budmoth larvae feeding upon the larch foliage, and a parasitoid population living off the budmoth larvae. Predicting the dynamics of such population systems with possible variations, extinctions, and interactions at multiple levels is a major challenge. We show here how the mere presence of additional parasitoid populations (having no direct mutual interactions) in the system can bring about drastic changes in the dynamics such as cessation of the cyclic outbreaks, or production of periodic population bursts. This also causes an increase in the time period of the budmoth cyclic outbreaks. Our model which also includes parameters to mimic environmental effects reproduces the 8–9 year cyclicity of budmoth outbreaks recorded over many years in the Swiss Alps, as well as variations from this recorded elsewhere. The populations survive extinction by increasing their numbers—a phenomenon termed the hydra effect, which is also exhibited by our model. Introduction of multiple parasitoid species makes the system more realistic, also providing a possible explanation of why periodic outbreaks of budmoth infestation have failed to recur in some parts of the world. Inclusion of environmental parameters makes our model's predictability higher and closer to what is observed in nature.

I. INTRODUCTION

The longest recorded time series of any population cycle is of the larch budmoth which periodically causes large-scale defoliation of larch trees at high altitudes. The budmoth population cycles have been documented by many (see for example, Refs. 1–6 and references therein). The time series that span a period of 1200 years has 123 outbreaks[1] which were deciphered via dendrochronological studies and direct observations conducted in the Swiss Alps. The dominant frequency of budmoth outbreaks here is 9 years which have occurred at altitudes of 1500–2000 m above sea level.[3] Similar studies in the Tatra mountains in Carpathian ranges in Slovakia do not reveal any cyclic outbreaks.[2,3] Other parts of the world do have irregular cycles, low amplitude cycles, and some regions are devoid of larch budmoths implying a local extinction event.[3] In the Swiss Alps, the expected 9-year cyclic outbreak failed to occur in 1990; indeed, they have not recurred there so far after 1981, and this has been attributed in the literature to climate change due to global warming.[4] In an earlier work,[7] we were able to explain all the observations mentioned above including occurrences of and variations from the 9 year cycles and non-occurrences of cycles using a q-deformed tritrophic model incorporating climate parameters which we proposed. This formulation enabled us to capture the

a)Electronic mail: janaki05@gmail.com

dynamics of this ecological system whose future state depends upon its history and past events. The discrete time tritrophic model we proposed had three populations: the larch tree represented by the plant quality index (PQI), the budmoth larvae which defoliate the larch, and a parasitoid population which live and feed upon budmoth larvae.

In this communication, we substantially extend the model of larch budmoth (LBM) population cycles by adding, in the tritrophic model, multiple species of parasitoids which do not have any direct interactions mutually and with the first parasitoid. This has, to our knowledge, not been explored before in the literature in any mathematical model of this system. We uncover that the periodic cycles of the budmoth population which arise have longer time periods than those with just one parasitoid species—a feature in agreement with experimental observations of the system with three species which was sprayed with a bacillus to control the budmoth larval population.[5] We show that addition of the second parasitoid species produces drastic changes in the dynamics of the system: its mere presence produces bursting oscillations of the budmoth population and the larch needle lengths, and partial or complete cessation of all oscillations. Further, the system admits interesting co-existing states such as periodic spiking behaviour with oscillation death or periodic bursting oscillations with oscillation death. We propose the introduction of the second parasitoid as an alternative mechanism for the cessation of periodic outbreaks seen in the Swiss Alps after 1981. We illustrate our results by movies of the time series and bifurcation diagrams.

In Section II we briefly outline the concept of q-deformations. In Section III we describe the existing framework and motivate the readers to move towards a q-deformed model (Section IV), followed by a discussion on various parameters that affect the system. We introduce a second parasitoid species into the system and show that this results in an increase in the time period of the budmoth cyclic outbreaks, as also observed experimentally. Some very interesting dynamical phenomena which result are also discussed. In Section V we briefly mention results we get when we extend the model to include 5 parasitoids in the system. Our study is useful as surveys and experimental observations have shown the existence of several parasitoid species hosted by a budmoth larva. In Section VI we perform a detailed exploration of the parameter space of our q-deformed tritrophic system with one parasitoid species. This is aided through movies of bifurcation diagrams which enable viewing the dynamics with respect to two parameters at a time. The model is generally robust under parametric perturbations, a feature which was not seen in previous (undeformed) models. The Routh–Hurwitz (RH) criterion is used to discuss the stability of the system, followed by numerical analysis.

II. q DEFORMATIONS

The concept of q-deformed analogues of numbers and functions dates back to Euler[8] and Heine[9] and these were developed further by Jackson.[10,11] q deformed functions and numbers are useful in explaining several experimental observations. Examples in the literature include the work in Refs. 12–20.

q-deformation of numbers and functions may be motivated by considering the differential equation $\frac{dy}{dx} = y$ which has the solution $\ln y = x$ or $y = e^x$. The differential equation $\frac{dy}{dx} = y^q$ on the other hand has the solution, $y = [1 + (1-q)x]^{\frac{1}{1-q}} \equiv e_q^x$, which gives $x = \frac{y^{1-q}-1}{1-q} \equiv \ln_q y$. Thus, $y = e_q^x$ and $x = \ln_q y$ are generalized solutions and are respectively called the deformed exponential and deformed logarithm functions. As q $\to$ 1, the original exponential and logarithm functions are recovered. q-exponentials were discussed in the context of anomalous diffusion which was shown to arise from type-III intermittent chaos in deterministic systems.[12] This work was the first to report asymptotically anomalous diffusion in chaotic systems. Expanding e_q^x in a Taylor series around $x = 0$, a new deformation scheme for numbers was obtained[10] which was used by Tsallis[13]

$$x_q = \frac{x}{1 + (1-q)(1-x)} = \frac{\frac{x}{2-q}}{1 + \frac{q-1}{2-q}x}. \tag{1}$$

Here we make use of this deformation as it mimics some key ecological features, as explained in Section IV.

III. THE TRITROPHIC SYSTEM IN BRIEF

As their foliage is consumed by the budmoth, the larch trees show fluctuations in their biomass and nutritive content. The larch is therefore characterized by its quality or health using the plant quality index (PQI). This is an estimate of the nutritive content of the plant measured by the needle length L_t at time t, longer needles being deemed healthier. Since larch needles average about 15 mm in length, the PQI is represented by a dimensionless quantity Q_t

$$Q_t = \frac{L_t - 15}{15}. \tag{2}$$

The budmoth population density N_t is estimated by counting the number of larvae in a given mass of larch branches. The parasitoids P_t which live on the budmoth larvae are not counted manually, but are assumed to be certain proportion of the budmoth hosts.

Observations and a large body of work in the past to understand the budmoth population cycles have led to the necessity of having all three trophic levels for the observed cyclicity in the system: the larch trees, the budmoths, and the parasitoids acting as a control on the budmoths.[4,7,21–24]

There are two tritrophic models extant in the literature, both due to Turchin—one in which the intrinsic growth rate for the budmoth is constant and the second one in which it is dynamically generated.

The model[22] having a constant intrinsic growth rate λ for the budmoth, is described by the following equations:

$$N_{t+1} = \lambda N_t \frac{Q_t}{\delta + Q_t} \exp\left[-\beta N_t - \frac{aP_t}{1 + awP_t}\right]$$
$$P_{t+1} = bN_t\left\{1 - \exp\left[-\frac{aP_t}{1 + awP_t}\right]\right\}$$
$$Q_{t+1} = (1-\alpha)\left(1 - \frac{N_t}{\gamma + N_t}\right) + \alpha Q_t. \quad (3)$$

Here, δ denotes the half saturation constant for PQI, a is the parasitoid searching rate, β indicates the budmoth intraspecific competition, γ the half saturation constant for the budmoth uptake, and b denotes the number of viable parasitoid offspring produced by an infested host (budmoth) per generation. w is the parasitoid wasting time and its value can vary from 0 (when there is no time gap between two encounters with its prey) to ∞ (when it is unable to find its prey). The parameter α is the vulnerability of the plant to the attacks of the budmoth, the plant recovery being given by $1-\alpha$. α can be related to the memory of the previous growth of the larch and therefore has a relation with the nutrient content in the plant biomass at the end of the previous infestation by the budmoths.

The budmoth population dynamics is governed by a Ricker[26] like growth term and a Nicholson–Bailey[27] type term modelling its interaction with the parasitoid. The variation in the growth rate is captured by λ multiplying a density dependent feeding that uses a Holling type-2 function.[28] This model was simulated using dimensionless scaling[29] and the parameter values from Turchin's work.[21,29] Although 9 year cycles were generated, the model is not robust under small variations in the parameters. In Turchin's other model[21] where the budmoth intrinsic growth rate is dynamically generated, the equations for P_t and Q_t remain as before but the budmoth equation is different

$$N_{t+1} = N_t \exp\left\{r_0\left(1 - e^{-\frac{Q_t}{\delta}}\right) - \frac{r_0}{K}N_t - \frac{aP_t}{1 + awP_t}\right\}, \quad (4)$$

where K is the carrying capacity of the budmoth and r_0 is the intrinsic growth rate at the first time step when the system just begins to evolve. The values of various parameters used in Ref. 21 are shown in Table I. This model also yields 9 year cycles as stated;[21] however, even a small variation of parameters within the error bars shown produce completely different periodicities.

IV. *q*-DEFORMED MODEL WITH TWO PARASITOIDS

The budmoth tritrophic ecological system is one which bears memory of previous year's growth. The growth of fresh larch needles, the nutrition present therein, and the population density of the infesting budmoths are related to each other in a rather complex manner. This is because the extent to which the larch foliage spreads depends upon the extent to which the trees have recovered from the infestation of the previous cycle of budmoths, which in turn depends upon the quality of larch needles and their availability then extant, as well as, additionally, the extent to which parasitoids have consumed budmoth larvae, etc. The probability of the system being in any given state is no longer the same for all states, since memory of the previously available resources of larch foliage, the previous plant quality index, the previous population densities of the budmoths as well as of the parasitoids all contribute to a current probability distribution; some probabilities are enhanced while others are suppressed. Hence, instead of considering this ecological system as a simple, ergodic one, it is much more apt to view it as a q-deformed system, in which, depending upon the value of q, probabilities of occurrences of events would be enhanced or suppressed.

TABLE I. Parameters used in Turchin's model-I.

Parameter	Range	Parameter	Range
r_0	2.5 ± 0.2	a	2.5 ± 1
α	0.5 ± 0.1	w	0.17 ± 0.2
K	250 ± 50	c	0.7 ± 0.2
δ	0.22 ± 0.05	d	150 ± 150

We use q-deformed variables to describe the populations in the system. Since each organism may respond differently to stimuli, one can assume distinct values of deformation parameter q_i for each species i. For simplicity, we make the choice: $q_x = 1$ for budmoth population density x, so that $x_q = x$. We introduce q-deformed variables[13] for the parasitoids and PQI for the following reasons. An assumption[30] usually made that the host density (budmoth larvae) is completely converted into parasitoid density just as in the Lotka–Volterra interaction[31–33] results in over-counting of the parasitoid numbers. The hyperbolic (Holling type-2) functional response avoids this overcounting. In our q-deformed model, the overcounting is avoided by taking $q_{parasitoid} \neq 1$. In the PQI equation, there is a need for incorporating density dependence of removal of the larch needles. This may be seen as follows. The wasteful feeding by the budmoths results in a lot of damaged foliage which then evolve in time depending upon environmental conditions. For low PQI, budmoth feed on whatever foliage is available, whereas for large PQI, budmoth consumption first rises and then attains saturation—thus at any given time, the availability of PQI (including partially consumed or damaged needles) is density dependent. This biologically true feature of density dependent removal of foliage (which is absent in the other models in the literature) is captured in our models (see also Refs. 7 and 39) by q-deformation in the z variable, i.e., by taking $q_{PQI} \neq 1$ in the PQI equation.

There are about 94 species of parasitoids which affect the larch budmoth.[24] It was reported after several surveys by Mills[25] that a budmoth can host an average of as many as 5.4 parasitoid species in an Upper Engadine site in any one year. The various parasitoids and the host form a parasitoid complex. The parasitoids attack the budmoth host during the various stages of the budmoth's life. Some parasitoids live in the larval stage of host, while some live their lives from the larval stage of the budmoth until the budmoth's pupal stage. Thus various interactions are possible in a parasitoid complex.

The larch budmoth can hence host many parasitoids or bacteria simultaneously. It has also been reported in Ref. 5

that bacterial sprays sprayed on budmoth larvae had the effect of increasing the time taken to attain the peak of the periodic infestation outbreaks.

To study the effect of the presence of an additional parasitoid species in the model, we consider first a simple situation where there are 4 interacting species: the larch budmoth population density (represented by x), the larch tree (represented by the PQI z), and population densities y and v of two species of parasitoids. The populations y and v do not interact with each other, though they both feed on the budmoth larvae. The equations in dimensionless form for this four-dimensional system at time t are

$$x_{t+1} = \frac{\rho_z z_t}{1+\mu_z z_t}\lambda x_t \exp\left(-x_t - \frac{\rho_y y_t}{1+\mu_y y_t} - \frac{\rho_v v_t}{1+\mu_v v_t}\right), \quad (5)$$

$$y_{t+1} = c x_t \left(1 - \exp\left(-\frac{\rho_y y_t}{1+\mu_y y_t}\right)\right), \quad (6)$$

$$v_{t+1} = \kappa c x_t \left(1 - \exp\left(-\frac{\rho_v v_t}{1+\mu_v v_t}\right)\right), \quad (7)$$

$$z_{t+1} = (1-\alpha)\left(1 - \frac{x_t}{m+x_t}\right) + \alpha(h - s x_t)\frac{\rho_z z_t}{1+\mu_z z_t}, \quad (8)$$

$$\mu_i = \frac{q_i - 1}{2 - q_i} \quad \rho_i = \frac{1}{2-q_i}, \quad (i = y, v, z). \quad (9)$$

The dimensionless variables x_t, y_t, z_t are related to N_t, P_t, and Q_t of Equations (3) and (4) through the transformations: $x_t = \beta N_t$, $y_t = aP_t$, and $Q_t = z_t$.

Here, $c = \frac{ab}{\beta}$ indicates the efficiency of the parasitoid in capturing its host among the available hosts. Thus, c indicates how well the parasitoid performs and how well its population density increases. The quantity $m = \beta\gamma$ is a measure of the efficiency of the budmoth in devouring the larch needles. The parameter κ decides which of the two parasitoids is stronger. When $\kappa = 1$ both parasitoids have the same virulence and fecundity. For $\kappa < 1$ the parasitoid v is weaker, while for $\kappa > 1$ parasitoid y is weaker than v. h and s are climate parameters which we had introduced in Ref. 7 to incorporate the effects of environment[34–37] on the (3-dimensional) system having just one parasitoid species. It has been noted that favourable environments play a vital role during recovery of larch trees after an infestation. If environmental conditions are good, the larch trees recover; else they do not, and the resulting needles are shorter, bulkier, and less nutritious for the budmoth. s controls the rate at which foliage is removed.

The need for including environmental/climate effects which could alter the entire dynamics of ecosystems has been emphasized in the literature.[38]

Our equation for the plant quality index contains three terms—the first term for the evolution of leaves that are not affected, the second term which governs the decay of PQI that is affected, and the last term represents the removal of PQI by the budmoth. Because of the introduction of climatic factors, our model which we proposed in Ref. 7 successfully explained the collapse of the budmoth cyclic outbreaks in the Swiss Alps after 1981 and allowed the system to also have longer periodicities as well as loss of cyclic behaviour.

In an earlier work[39] we had related q_y to w: $\mu_y = \frac{q_y - 1}{2 - q_y} = w$. Since μ_y varies from 0 to ∞, q_y can vary from 1 to 2. Similarly we had related q_z to the budmoth intraspecific competition coefficient β: $q_z = 1 + \beta$, from $\mu_z = \frac{1}{\delta}$ and $\rho_z = \frac{1}{\beta\delta}$. q_z is also restricted to vary between 1 and 2.

Our earlier model[39] was designed to bring in a density dependent removal of the larch needles through the term $\alpha z_{q_t} x$ in place of their constant removal which is in Turchin's models. This corresponds to the situation $s = 1$, $h = 0$ of our later model in Ref. 7.

That model[39] (without a factor for evolution of damaged leaves), however, is suited to situations where the devoured leaves do not sprout back. This can happen when the trees are destroyed beyond repair. This is seen in the French Alps, where human intervention (in the form of logging for timber, conversion of forest land to pastoral grounds, etc.) has resulted in a permanent destruction of larches.[6]

In Turchin's model parameters such as w (related to q_y in our model), δ (related to q_z in our model), m, c, α cannot change as they are species-specific. Only long term forces like evolution can change them. Thus the only parameter that is truly free to vary in that model is λ. Our model in Equations (5)–(9) has 3 other free parameters: h, s, and κ.

The stability of our 4-dimensional system is studied using the Routh–Hurwitz criterion. We discuss this in the Appendix; it is seen that both the single parasitoid system ($\kappa = 0$) and one with two parasitoids ($\kappa \neq 0$) admit limit cycles in certain parameter regimes. The system with four interacting species presents very interesting behaviour: while in some regimes show cyclic behaviour, others exhibit periodic bursting behaviour. In certain domains there is both partial and complete amplitude death, or co-existence of bursting and oscillation death.

In all figures in this paper, we have used the following notation: LBM denoting the budmoth population density x, PQI standing for the plant quality index z, "Parasitoid 1" denoting y, "Parasitoid 2" denoting v, etc.

A. Oscillation quenching in the 4-dimensional system

Destruction of oscillations can occur via amplitude death or oscillation death.[40] Whereas in amplitude death cycles die and reach a steady (homogeneous) state, in the case of oscillation death the final state is inhomogeneous. In Ref. 40 situations were discussed where both amplitude and oscillation deaths occur due to a direct coupling between the oscillators, and the coupling strength plays a vital role in quenching the oscillations—all the interacting species underwent decay of oscillations. It was emphasized in Ref. 40 that co-existence of attractors (both limit cycles and steady states in its phase space) is required for oscillation death to occur.

In our 4-dimensional system with 2 parasitoids, there is no diffusive or direct coupling between the variables as in the situations discussed in Ref. 40 but rather, it occurs in the exponential, in the budmoth equation, through differences of the q-deformed variables y and v. The coupling parameter here is κ, which compares the strengths or efficiencies of the two parasitoids in infesting the budmoths. Higher the value of κ greater is the infesting ability of the second parasitoid.

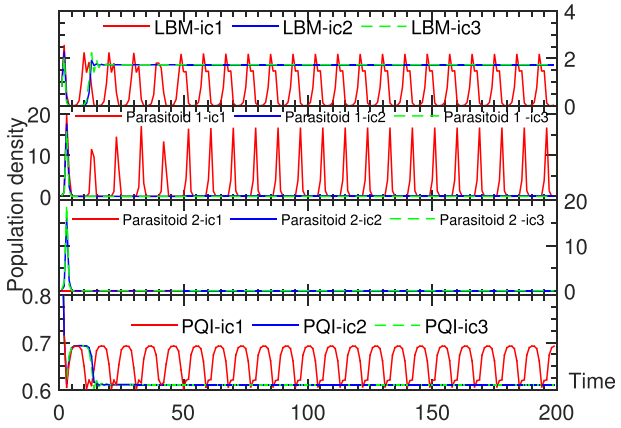

FIG. 1. Co-existence of attractors in the 4-d system ($q_y = q_v = 1.13$, $q_z = 1.34, \alpha = 0.5, c = 12, m = 13, h = 0.5, s = 0.01, \lambda = 8.0, \kappa = 0.95$) for 3 different initial conditions (ic1, ic2, ic3). (i) ic1: $x_0 = 0.8$, $z_0 = 1$, $y_0 = 0.1$, $v_0 = 0.0$ (red), (ii) ic2: $x_0 = 0.8, z_0 = 1, y_0 = 0.1, v_0 = 0.1$ (blue), and (iii) ic3: $x_0 = 0.8, z_0 = 1, y_0 = 0.1, v_0 = 0.2$ (green). In this example, when $v_0 \neq 0$ (green and blue), cycles of all 3 species are destroyed. $v_0 = 0$ is the 3-population tritrophic model.

Bursting behaviour is seen for the budmoth population and the PQI in several parameter regimes. For different values of κ and other parameters, different kinds of interesting behaviours emerge.

1. Co-existence of attractors

The system is very sensitive to initial conditions as different initial conditions land it in different parts of the phase space. A representation of this is seen in Figs. 1 and 2, where the evolution of the system is shown for three different initial conditions; co-existing solutions are clearly seen. This is also clearly demonstrated in the accompanying supplementary multimedia movie file showing co-existing solutions. It is seen in two of the solutions (see Fig. 1) that the

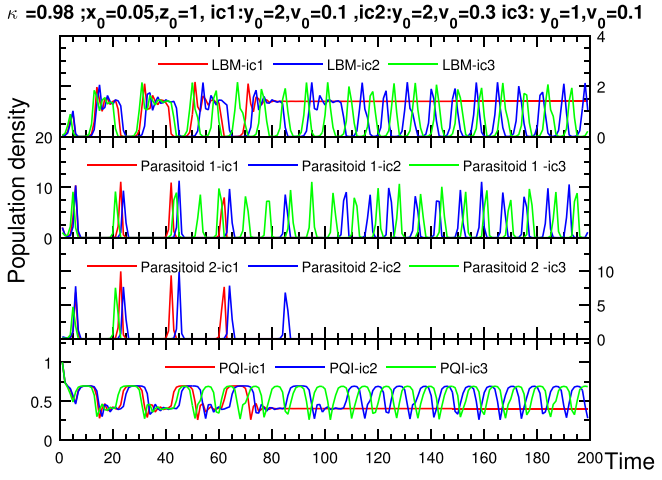

FIG. 2. Screenshot of a time series video for 3 different initial conditions showing amplitude death in parasitoid species y and v of the 4-d system obtained by varying κ from 0 to 2. Parameter values: $q_y = q_v = 1.13$, $q_z = 1.34, \alpha = 0.5, c = 12, m = 13, h = 0.5, s = 0.5, \lambda = 8.0$ with different initial conditions (ic1, ic2, ic3). (i) ic1: $x_0 = 0.05, z_0 = 1, y_0 = 2, v_0 = 0.1$ (red), (ii) ic2: $x_0 = 0.05, z_0 = 1, y_0 = 2, v_0 = 0.3$ (blue), and (iii) ic3: $x_0 = 0.05, z_0 = 1, y_0 = 1, v_0 = 0.1$ (green). Different initial conditions evolve differently. (Multimedia view) [URL: http://dx.doi.org/10.1063/1.4962633.1]

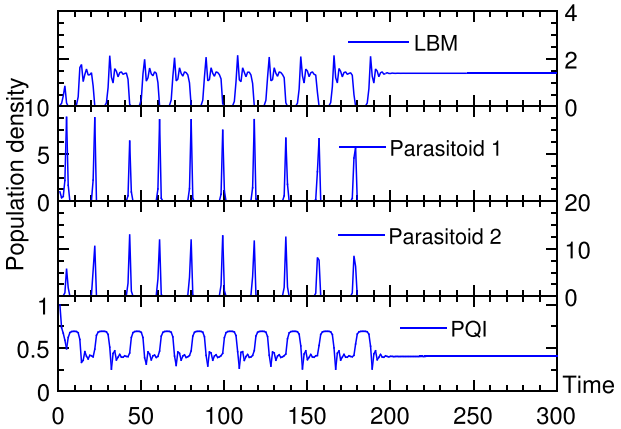

FIG. 3. Oscillation death in all four species (parameter values and initial conditions: $q_y = q_v = 1.13, q_z = 1.34, \alpha = 0.5, c = 12, m = 13, h = 0.5, s = 0.5, \lambda = 8.0, \kappa = 1.07, x_0 = 0.05, y_0 = 1, z_0 = 1, v_0 = 0.1$).

presence of the second parasitoid destroys oscillations in the system.

2. Oscillation death and amplitude death

In Fig. 3 it is seen that all the four species oscillate for sometime before experiencing complete death of oscillations. In particular, the budmoth population and PQI shows bursting behaviour. For the parameters used in Fig. 4, all four species oscillate when $0.56 < \kappa < 1.84$. However, for $\kappa \leq 0.56$ and $\kappa \geq 1.84$ one of the parasitoids is completely wiped out: the mere presence of one parasitoid drives the other to extinction. The introduction of a second virulent parasitoid causes more casualty of the host. Due to the increase in loss of the host, the first parasitoid gradually diminishes in number and becomes extinct, while the second one is able to survive on low host numbers. It should also be noted that the fecundity of the virulent host is higher, as c is proportional to the number of surviving parasitoids that are produced. This is also seen in the bifurcation diagram of the budmoth density with respect to κ (Fig. 5). One can see domains of

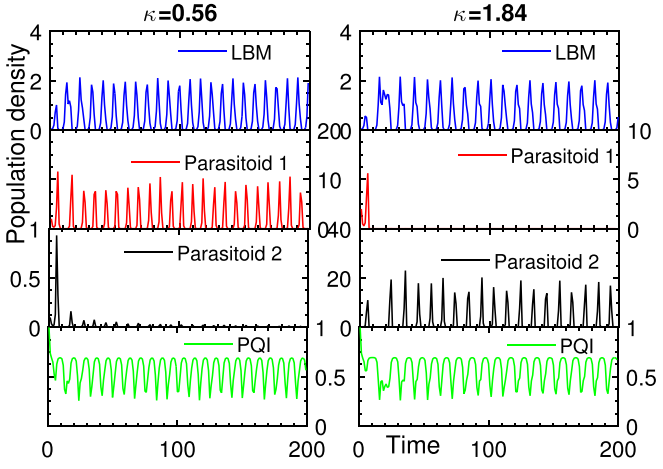

FIG. 4. Partial amplitude death in the 4-d system: When κ is changed, amplitude death occurs in one species alone. Left panels: $\kappa = 0.56$; right panels: $\kappa = 1.84$. Other parameters: $q_y = q_v = 1.13$, $q_z = 1.34$, $\alpha = 0.5$, $c = 12$, $m = 13$, $h = 0.5$, $s = 0.5$, $\lambda = 8.0$. Initial conditions: $x_0 = 0.05$, $z_0 = 1$, $y_0 = 2$, $v_0 = 0.1$.

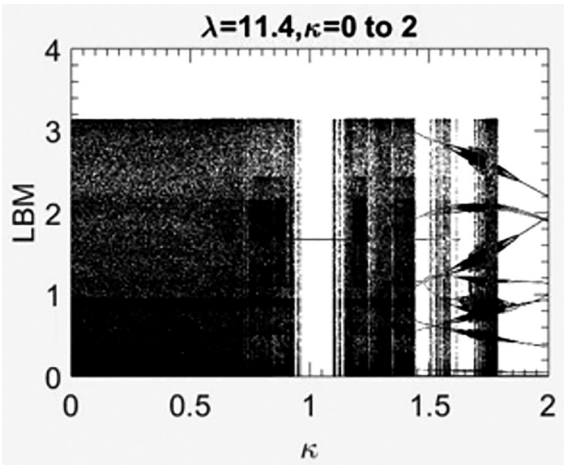

FIG. 5. Screenshot of a bifurcation diagram video with respect to κ for varying λ. ($m=13$, $c=12$, $\alpha=0.5$, $h=0.5$, $s=0.5$, $q_y=1.13$, $q_v=1.13$, $q_z=1.34$). (Multimedia view) [URL: http://dx.doi.org/10.1063/1.4962633.2]

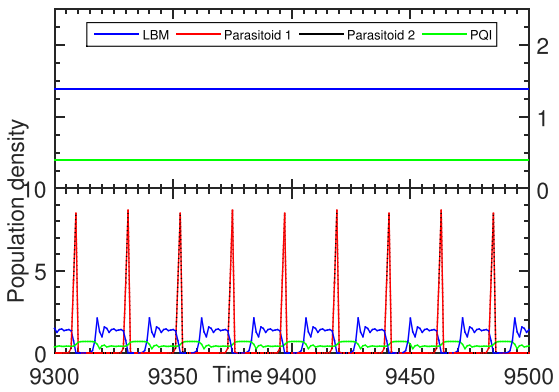

FIG. 6. Co-existing solutions in the 4-d system for $\kappa=1$, $\alpha=0.5$, $c=12$, $m=13$, $h=0.5$, $s=0.5$, $\lambda=8.0$, $q_y=q_v=1.13$, $q_z=1.34$. Top panel: Both parasitoids show amplitude death for initial conditions: $x_0=0.05$, $z_0=1.0$, $y_0=2.0$, $v_0=0.1$. Bottom panel: Both parasitoids show completely synchronized periodic oscillations for initial conditions: $x_0=2.6540$, $z_0=0.2082$, $y_0=0.2135$, $v_0=1.4653$.

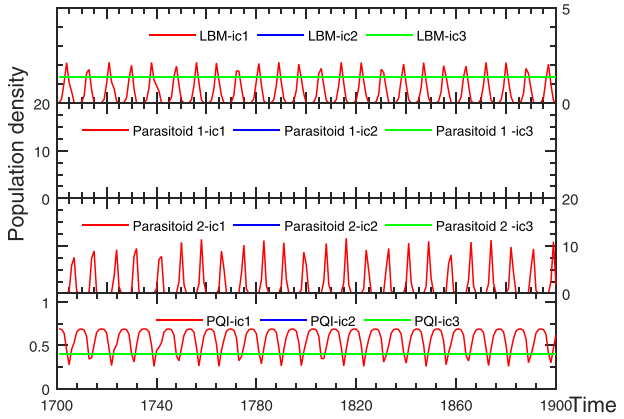

FIG. 7. Co-existing spiking and fixed point solutions for the 4-d system for $\kappa=1.06$, $\alpha=0.5$, $c=12$, $m=13$, $h=0.5$, $s=0.5$, $\lambda=8.0$, $q_y=q_v=1.13$, $q_z=1.34$. Different initial conditions are: (i) $x_0=0.05, z_0=1, y_0=2, v_0=0.1$ (red), (ii) $x_0=0.05, z_0=1, y_0=2, v_0=0.3$ (blue), and (iii) $x_0=0.05, z_0=1, y_0=1, v_0=0.1$ (green).

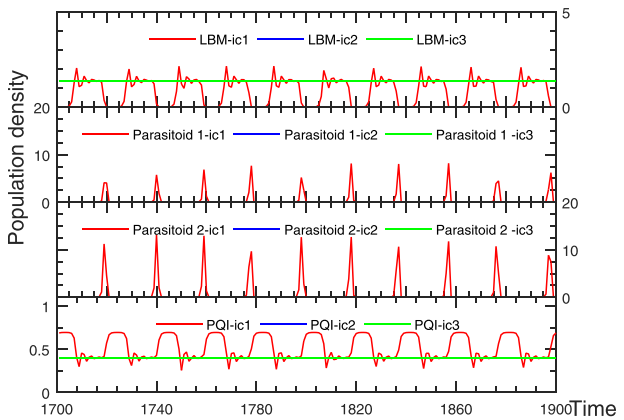

FIG. 8. Co-existing bursting and fixed point solutions for the 4-d system for $\kappa=1.08$, $\alpha=0.5$, $c=12$, $m=13$, $h=0.5$, $s=0.5$, $\lambda=8.0$, $q_y=q_v=1.13$, $q_z=1.34$. Different initial conditions are: (i) $x_0=0.05, z_0=1, y_0=2, v_0=0.1$ (red), (ii) $x_0=0.05, z_0=1, y_0=2, v_0=0.3$ (blue), and (iii) $x_0=0.05, z_0=1, y_0=1, v_0=0.1$ (green).

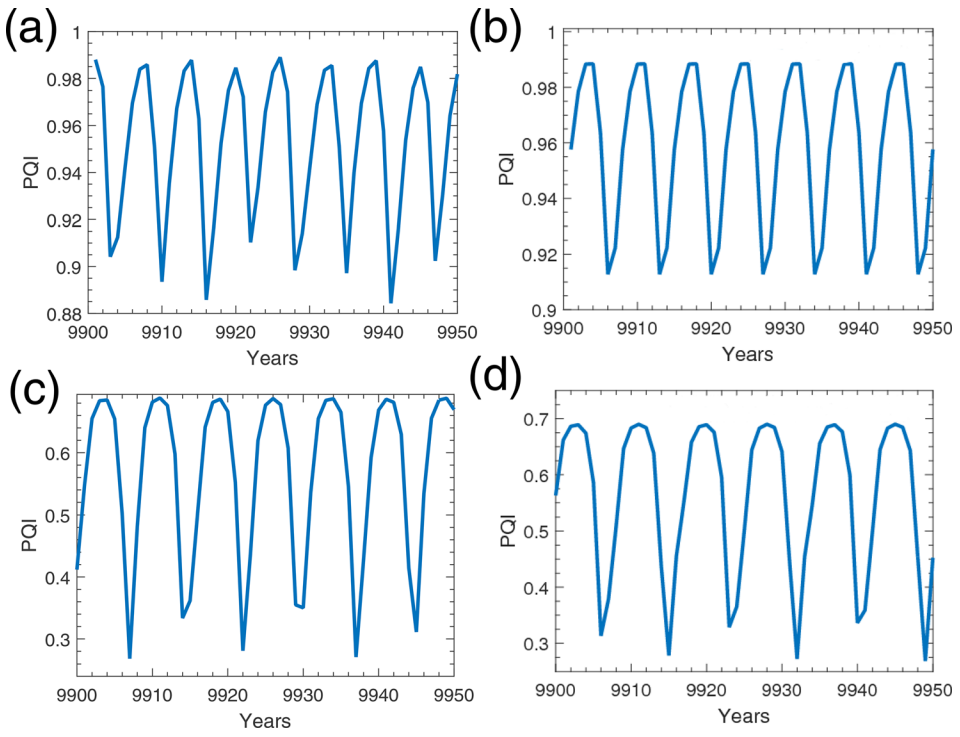

FIG. 9. Variation in PQI obtained from (a) Turchin's model-1 with 1 parasitoid species; (b) Turchin's model-1 in which we have added a 2nd parasitoid species; (c) our q-deformed model with 1 parasitoid species; (d) our q-deformed model with 2 parasitoid species (Eqs. (5)–(9). Both (a) and (b) show a very small needle-length variation which is unrealistic while both (c) and (d) show a significant variation in the lengths as seen in nature. Note the different scales on the y-axis.

oscillation death and oscillating solutions as κ varies. Although both parasitoids do not mutually interact directly, one of them pushes the other out. This is manifested as partial amplitude death in our system.

3. Co-existence of periodic oscillations and amplitude death for $\kappa = 1$

When the virulence of the parasitoids is comparable, i.e., when $\kappa = 1$, we interestingly get a situation of co-existence. While most of the initial conditions lead to oscillation death of the PQI and budmoth population, and amplitude death of both parasitoid populations, a smaller percentage of the initial conditions produce periodic bursting in the budmoth population and PQI, and mutually completely synchronized periodic oscillations in both the parasitoids (Fig. 6). This is extremely interesting as this provides a possible explanation for the cessation and non-recurrence of the regular 9 year periodic budmoth outbreaks in the Swiss Alps after 1981 for the first time after 1200 years.[1] Also, the variations in the periodicity of the outbreaks seen in the French Alps[6] and the historical absence of cycles in the Carpathian Tatra mountains could be attributed to the presence of a second parasitoid species in the system. Figures 7 and 8 illustrate the co-existence of spiking and bursting solutions, respectively, with fixed point solutions—very small variations in κ change normal periodic behaviour to periodic bursting. From Fig. 8 it is seen that as the budmoth population rises the PQI falls and vice versa, and when the budmoth population oscillates about the fixed point solution, so does the PQI. The population densities of the parasitoids begin to peak when the budmoth population is at its maximum and fall when the budmoth population is nearly zero—the oscillations of the four species show synchronized behaviour, and as previously stated, bursting oscillations occur only for some range of κ values. All these observations are clearly seen in the supplementary multimedia video file linked to Fig. 2.

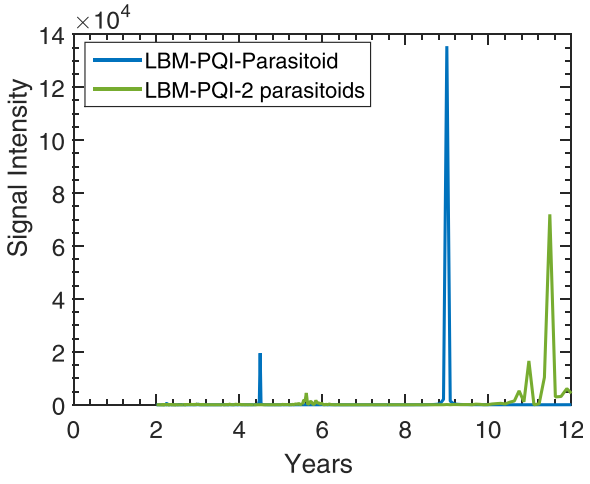

FIG. 10. Addition of a second parasitoid in the system increases the time period of budmoth outbreaks. 3-d model (1 parasitoid) is shown in blue, and 4-d model (2 parasitoids) is shown in green. Parameters: $q_y = q_v = 1.13$, $q_z = 1.34$, $\alpha = 0.5$, $c = 12$, $m = 13$, $h = 0.5$, $s = 0.5$, $\lambda = 6.5$, $\kappa = 1.95$. Initial conditions: $x_0 = 0.5$, $y_0 = 1.7$, $z_0 = 1$, $v_0 = 0.2$. The time period is shifted by almost 2 years.

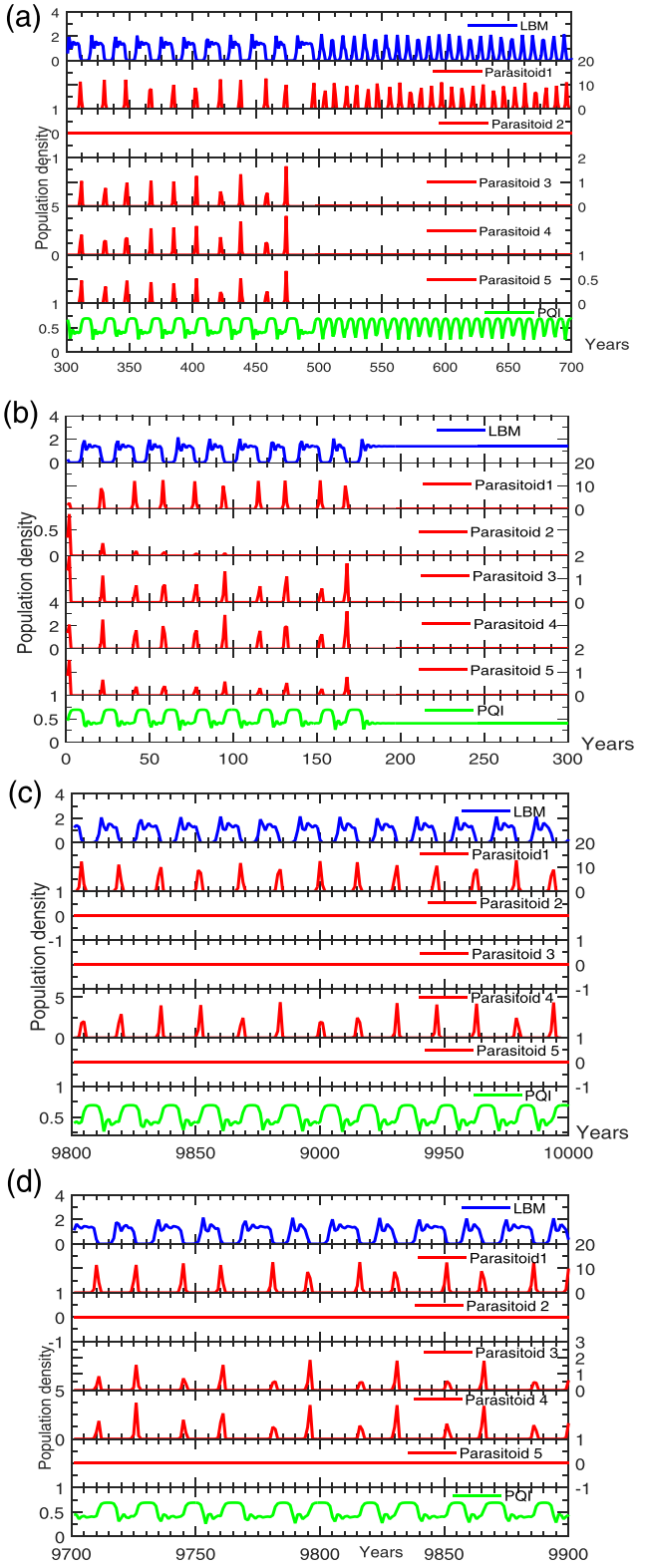

FIG. 11. Time series showing different dynamical behaviour for different initial conditions for the 7-d system (five parasitoid species) Parameters: $q_i = 1.13$, $m = 13$, $c = 12, q_z = 1.34$, $\alpha = 0.5$, $h = 0.5$, $s = 0.5$, $\kappa_1 = 0.75$, $\kappa_2 = 0.8$, $\kappa_3 = 0.84$, and $\kappa_4 = 0.78$. Initial Conditions: (a) $x_0 = 0.2134$, $y_0 = 1.2576$, $z_0 = 0.4577$, $p_0 = 0.7182$, $u_0 = 3.7462$, $v_0 = 0.0087$, $w_0 = 1.9486$ (Bursting and spiking); (b) $x_0 = 0.2828, y_0 = 1.6414, z_0 = 0.4556$, $p_0 = 0.8392$, $u_0 = 1.3592$, $v_0 = 0.3463, w_0 = 1.3630$ (oscillation death); (c) $x_0 = 0.0856$, $y_0 = 2.9617$, $z_0 = 0.5574$, $p_0 = 4.1272$, $u_0 = 0.5562$, $v_0 = 0.4435$, $w_0 = 2.1998$ (Bursting in budmoth and PQI); (d) $x_0 = 0.4002$, $y_0 = 1.0858$, $z_0 = 0.6006$, $p_0 = 0.0670$, $u_0 = 2.5175$, $v_0 = 0.2879$, $w_0 = 2.2384$ (Bursting with alternate 2-spike and 3-spike bursts).

An important point to bear in mind is that a defoliation event would be expected to result in a considerable variation in the needle lengths. This is also consistent with observations as cyclic defoliation leads to cyclic browning of larch forests. However, the PQI in Turchin's (scaled) models does not show much variation although it exhibits cycles. Moreover, it always maintains a very high value which is unrealistic because actual observations show a large variation. Those models do not produce small needle lengths characterizing heavy defoliations. Our q-deformed model mimics actual observations and produces significant variations in needle lengths. A comparison of the variation in PQI obtained from Turchin's model and that from our q-deformed model is given in Fig. 9 (note the different scales on the y-axis).

4. Effect of the second parasitoid on the time period

Due to the presence of the second parasitoid, the time period of the system increases as depicted in Fig. 10. This is understandable as the budmoth is now additionally under attack by the second parasitoid species, so that it takes longer to recover its peak value of population density. This is in agreement with results of experiments[5] where a bacillus (corresponding to parasitoid 2) was sprayed over the budmoth resulting in an increase of the time period of the budmoth outbreak.

We therefore propose that changes (increases) in the time period of recurrence of budmoth outbreaks observed at different times in different parts of the world could also be due to the presence of a second parasitoid species infesting the larch budmoths.

V. GENERALIZATION TO 5 PARASITOID SPECIES (7-d SYSTEM)

As mentioned in Section IV, it has been reported in Ref. 25 that a budmoth in the Upper Engadine area of the Swiss Alps is known to host an average of 5.4 parasitoid species in a year. It is therefore interesting to know the dynamics which our q-deformed model exhibits when say, five parasitoid species are present at a given time on a budmoth. We repeated the simulations of our model (Eqs. (5)–(9)) for 5 parasitoids. Introducing each new parasitoid species brings in 2 parameters: κ_i, and q_i the parasitoid wasting time ($i = 1, 2, 3, 4$ denoting the additional parasitoid species p, u, v, w respectively). Adding a 5th parasitoid species produces cycles for certain values of initial conditions. However if the initial conditions are such that any one parasitoid species has a large number density, the system undergoes an oscillation death for the budmoth and PQI while all the parasitoid

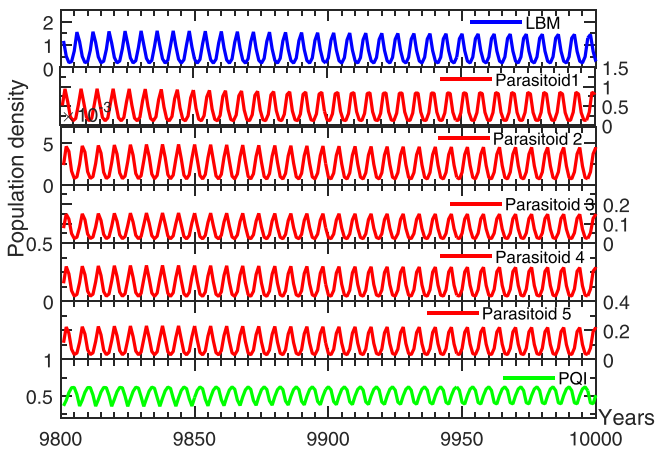

FIG. 12. Co-existence of all 7 species, all exhibiting cycles. Parameters: $c = 1.9, h = 0.5$, $s = 0.5$, $q_y = 1.13$, $m = 13$, $\alpha = 0.5$, $q_z = 1.34$, $\kappa_1 = 0.78$, $\kappa_2 = 0.8$, $\kappa_3 = 0.84$, $\kappa_4 = 0.82$. Initial conditions: $x_0 = 0.2940$, $y_0 = 0.6270$, $z_0 = 0.1959, w_0 = 0.3317, v_0 = 0.3679, p_0 = 0.5663, u_0 = 0.2088$.

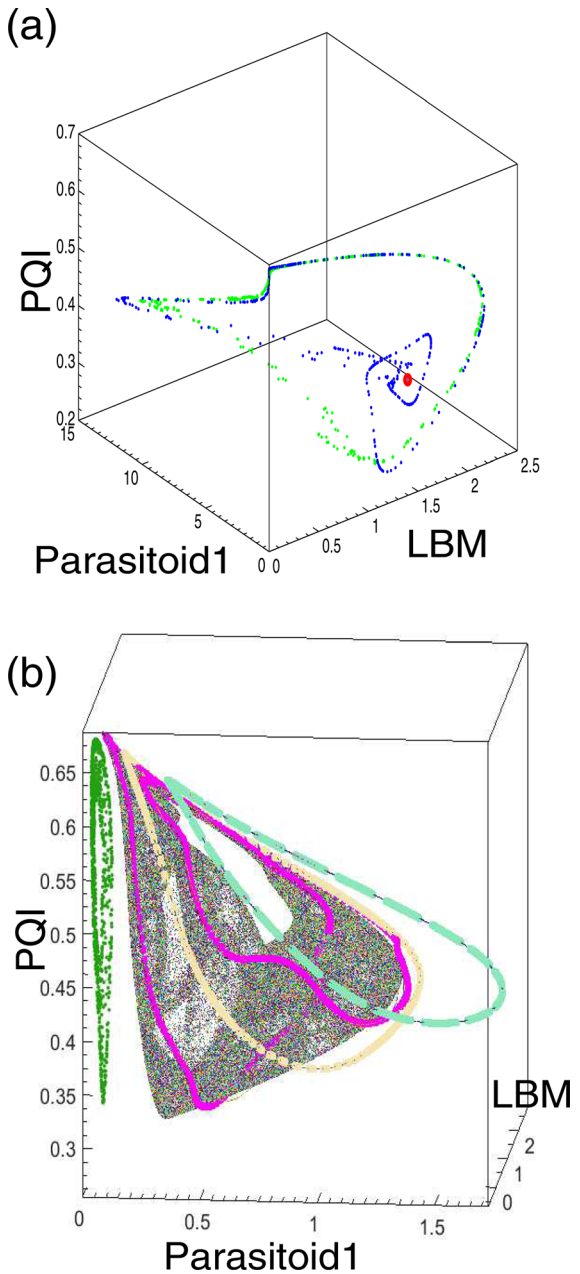

FIG. 13. Attractors for the 7-d system. Parameters: $q_i = 1.13$, $m = 13$, $q_z = 1.34$, $\alpha = 0.5$, $h = 0.5$, $s = 0.5$, $\kappa_1 = 0.75$, $\kappa_2 = 0.8$, $\kappa_3 = 0.84$, $\kappa_4 = 0.78$. (a) $c = 12$. Three closely spaced attractors can be seen—the green one corresponds to spiking behaviour, the blue one corresponds to bursting behaviour, and the third attractor is a stable fixed point shown in red. This was originally plotted using 2000 initial conditions. However, for the sake of visual clarity only 100 initial conditions are shown here; (b) $c = 2.25$. Here 5 closely lying attractors are seen (coloured in green, grey, magenta, light-blue, and mauve). The system was run for 10 000 iterations and the last 1000 points were used to generate the plot. 1000 random initial conditions were used.

populations undergo an amplitude death. The system is highly parameter dependent and shows a variety of dynamical behaviour. Shown in Figures 11 and 12 are some representative time series.

For the simulations we have given all the parasitoids the same value for the wasting time; this still leaves four values of κ_i which must be adjusted along with the initial conditions to have a specific behaviour. In our simulations we have checked 500 random initial conditions that give rise to cyclic behaviour. Fig. 11(d) shows an interesting bursting behaviour with alternate 2-spike and 3-spike bursting. In certain other parameter domains irregular bursts are generated (not shown). One needs to exhaustively explore the parameter space to know of all the dynamical possibilities as ecological systems involve a multitude of complex interactions. We see sensitive dependence to initial conditions. Stable cycles exist for certain values of the initial conditions, while certain initial conditions lead to some parasitoids being wiped out. In certain parameter domains, all species co-exist and exhibit cycles (Fig. 12). For bursting to occur in the budmoth and PQI, we observe that at least 2 parasitoid species have to co-exist for the larch budmoth system. A 3-dimensional projection of the attractor for the 7-dimensional system (5 parasitoids) is plotted in Fig. 13 for 2 different values of c. Fig. 13(a) (for $c = 12$) shows that spiking and bursting dynamics belong to different basins of attraction. Different initial conditions belonging to the different basins of attraction go to different attractors—one for spiking behaviour, one for bursting dynamics, and the third is a fixed point—and this illustrates the non-ergodicity of the larch budmoth system. Introduction of each new species brings in more complexity. Fig. 13(b) shows existence of multiple (five) attractors for a lower c value ($c = 2.25$) for this 7-dimensional system. The consequent expansion of the parameter space implies that now there is more stringency in the choice of the parameter values for reproducing the same dynamics that occurred for the lower dimensional case. Cycles that occurred so easily in our three dimensional system (with 1 parasitoid species) become more and more rare with the same parameter set as we add more and more species.

VI. THE SPECIAL CASE $\kappa = 0$ (3-d SYSTEM)

A. Neimark–Sacker bifurcation

Numerical simulations confirm the creation of limit cycles via a Neimark–Sacker bifurcation. As the parameter c or λ is varied, the stable fixed point becomes a stable spiral which loses its stability and a limit cycle is born surrounding it. These stable limit cycles manifest as population cycles. We see from the time series and the bifurcation diagrams that there is synchrony between the three interacting species. Fig. 14 shows a Neimark–Sacker bifurcation with respect to parameter λ. The inset (c) in Fig. 14 exhibits the stable fixed points turning into stable spirals as λ increases. Stable limit cycles are born for λ increasing beyond 1.9; further increase in its value results in the creation of limit cycles with larger amplitudes. Fig. 15 similarly demonstrates the formation of limit cycles as c is varied; the topmost image shows limit cycles for the 3-dimensional system with one parasitoid species ($\kappa = 0$), the middle one for the situation $\kappa = 1$ when both parasitoids have identical virulence and fecundity, while the bottom plot shows limit cycles for $\kappa = 1.95$.

B. Bifurcation diagram videos with 2 varying parameters

We generated bifurcation diagrams for the system when two parameters say (i, j), $(i, j = h, s, \alpha, \lambda, c, m, q_y, q_z)$ vary simultaneously, in the form of videos (see supplementary multimedia files).

As the parameter i is varied, the bifurcation diagram with respect to different values of j are calculated and stored. As the movie is played, each frame corresponds to a different

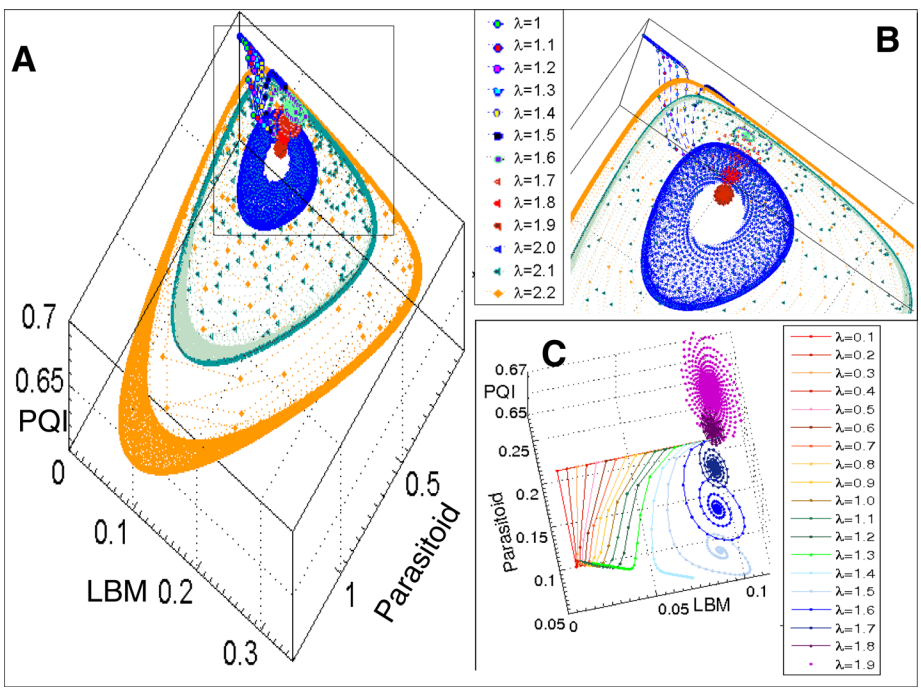

FIG. 14. Neimark–Sacker Bifurcation with respect to λ in the 3-d system (one parasitoid species) keeping other values fixed at $q_y = 1.13$, $m = 13$, $c = 12$, $q_z = 1.34$, $\alpha = 0.5$, $h = 0.5$, and $s = 0.5$.

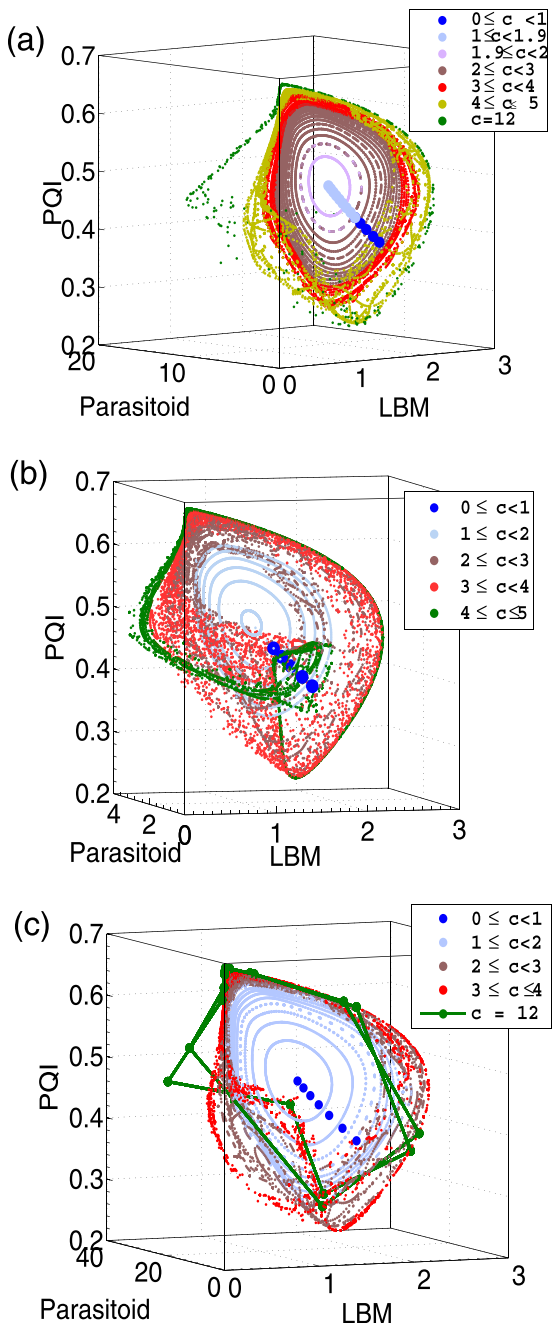

FIG. 15. Neimark–Sacker bifurcation with respect to c keeping other values fixed at $q_y = 1.13, m = 13, \lambda = 8, q_z = 1.34, \alpha = 0.5, h = 0.5$, and $s = 0.5$ for (a) $\kappa = 0$ (3-d system); (b) $\kappa = 1, q_y = 1.13$ (c) $\kappa = 1.95, q_y = 1.13$.

i having a bifurcation diagram with respect to j. There are 8 parameters in the system; hence, taking two at a time results in 56 combinations. The results of these bifurcation videos are shown in Table III. Table II provides a guide for reading Table III. It is seen that a Neimark–Sacker bifurcation occurs with respect to all parameters.

C. Chaotic bubbles and multistability

There is an intriguing presence of bubbles, including chaotic bubbles, in the bifurcation diagrams with respect to all the parameters in the system except c, q_y, and m. As bubbles are indicative of the hydra effect, a seemingly paradoxical phenomenon involving an increase in the population size of a species in response to an increased mortality rate,[41] our study indicates that several routes exist in our complex tritrophic system by which extinction of any of the three species may be avoided. This is particularly visible for variation with respect to α. When the plant recovery rate $1 - \alpha$ decreases with increasing α, the plant quality degrades slowly with increasing budmoth infestation, so that one expects complete destruction of the larch plant. However, the larch species does not actually die out, but rather springs back to life. The first instantaneous response to extreme stress on populations would be an increased growth rate. Increased stress/constraints on the system can induce more nonlinearities and variability in the time series than that in a system in the absence of constraints (such as infestation by a predator/parasite).[42] In our model, the parameters α, q_z, λ, h, and s, all affect the populations rapidly and therefore any variations in these could result in a situation reminiscent of the hydra effect. Fig. 16(a) shows the presence of several chaotic bubbles for $0.358 < h < 0.716$ which are created in the periodic window around $\alpha = 0.5$. Another interesting feature of the system is the occurrence of multistable states in different domains of the parameter space. Fig. 16 (right) shows the simultaneous presence of seven stable limit cycles between which the system hops at $c = 7$ and $q_z = 1.99$ (when the budmoth intraspecific competition is very high). The simultaneous existence of 7 stable limit cycles shows the various possibilities for the system of being in stable periodic states for a given parameter set. In Fig. 17 these limit cycles can be seen more clearly.

D. Influence of different parameters on the time period

Since the system is highly nonlinear, it is quite difficult to pinpoint accurately how the time period is affected. Keeping 7 parameters constant, the remaining one is varied and its effect on the time period is noted. In Fig. 18, we have plotted the trends obtained for the time period of budmoth outbreaks with a change in the parameters, generated by picking the frequency corresponding to the maximum power in the fast Fourier transform of the time series. (i) Numerically, we find that as λ increases, the time period decreases. This is understandable since the population increases faster with increasing growth rate, depleting the resources more rapidly which consequently causes a decline in the budmoth population resulting in smaller cycles. (ii) Similarly increasing h results in a good growth of larch foliage which leads to an improvement in the budmoth population followed by a quick depletion of available food again leading to its population decline, resulting in smaller cycles. (iii) s does not change the time period significantly except at very high values where the time period shows large fluctuations. (iv) As m is increased, the time period stabilizes around 9 years except for small fluctuations about this value. Thus, the way the budmoth feeds does not appear to have much effect on the system. (v) Increasing the value of c, the efficiency of the parasitoid in killing the budmoth, keeps the budmoth population in check, making it taking longer to

TABLE II. Abbreviations used in Table III.

PD/PH	Period doubling (1 into 2)/period halving (2 into 1)
NS/RNS	Neimark–Sacker bifurcation/reverse Neimark–Sacker bifurcation
PP	Periodic pattern
SRC/SNK	The region from where fixed points spread out (source)/annihilate (sink)
SB	Simple Bubble (closed structure formed by a PD,PH)
CB	Complex Bubble (formed via a few PD and PH)
Z	Any of the 8 parameters with respect to which the bifurcation diagram is generated
Z_c	The value of Z at which NS occurs
ChB	Chaotic bubble (many PD, PH chaos inside bubble)
Z_{max}	The value of Z at which BC occurs
CR/Ch	Chaotic region (fine distribution of points)/Chaos
DB/IB	Distorted bubble/Interlaced bubbles (many bubbles join)
BC	Boundary crisis (sudden disappearance of points after a Z)
Bfd	Bifurcation diagram
IC	Interior crisis (expansion or compression of size of attractor)
λ	Intrinsic growth rate ($0 \leq \lambda \leq 12$)
$\uparrow/\downarrow$	Increases/decreases
α	Plant vulnerability ($0 \leq \alpha \leq 1$)
h/s	Environmental factors ($0 \leq h, s \leq 1$)
$\rightarrow/\leftarrow$	Bfd shifting towards right/left (higher/lower values)
c	Efficiency of parasitoid ($0 \leq c \leq 15$)
$Z_>/Z_</X$	Greater/lesser values of parameter /No drastic change from the original configuration
m	Budmoth's efficiency of infesting($0 \leq m \leq 20$)
q_z/q_y	Intraspecific competition/parasitoid wasting time ($1 \leq q_z, q_y \leq 2$)
PW/CR/SB/ChB/CB	Periodic window/chaotic region/simple bubble/chaotic bubble/complex bubble
PW to CR	PW becomes SB, turns into CB and becomes ChB. Finally, CR of all bubbles form CR of the Bfd
Pop_{max}	Maximum population attained by the species
OD	Oscillation death

reach its peak value, thus increasing the time period. (vi) As the plant vulnerability α increases, the larch needles are quickly depleted due to heavy infestation. This results in the larch foliage taking longer to re-grow which makes the cycles longer and more difficult to attain if α takes very high values. (vii) As q_y related to the parasitoid wasting time increases, the budmoth numbers increase. This depletes larch foliage and the consequent reduction in available food brings down the budmoth population resulting in smaller cycles. (viii) There is not much change in the time period with respect to q_z. From the figures it is also clear that the 9 year cycles stay despite perturbations on the parameters. Thus our model is robust to small variations in the parameters, producing cycles of nearly the same periodicity which is also what is observed in nature. This may be contrasted with earlier models extant in the literature[21–23] where even a small change would give rise to a completely different time period.

VII. CONCLUSIONS

We have analysed here four and higher dimensional systems with two or more parasitoids. They display interesting

TABLE III. Analysis of bifurcations for the 3-d system with one parasitoid species. These videos were generated for value of $\alpha = 0.5$, $h = 0.5$, $s = 0.5$, $q_y = 1.13$, $q_z = 1.34$, $\lambda = 8$, $c = 12$, and $m = 13$. The entries i, j here represent the two parameters that are chosen to make the video. The parameters in the columns (j) are those on the abscissa of the bifurcation diagrams while the parameters in the rows (i) represent the parameters which are seen varying on the top in the videos.

	α	h	s	m	λ	c	q_y	q_z
α	…	$Pop_{max} \uparrow$ Satellites PW to CR	SNK at $s = 0.5$ $Pop_{max} \downarrow$ SB to CR CR to SB	Satellites SNK $8 < m < 15$	$Pop_{max} \uparrow$ $\lambda_c \uparrow$ SNK at $\lambda = 8$ $\lambda_{max} \downarrow$	$c_c \uparrow$ CR to PW $Pop_{max} \downarrow$ PW to CR	RNS $\uparrow$ $Pop_{max} \downarrow$ PW to CR CR to PW	$\rightarrow$ SNK at $q_z = 1.5$
h	CR to PW SNK at RNS	…	CR to PW Satellites	PW to CR CR to PW $Pop_{max} \uparrow$	RNS $\downarrow$ $\lambda_{max} \downarrow$ $\leftarrow$	$\rightarrow$Slow $Pop_{max} \uparrow$	X	$\leftarrow$ Satellites
s	RNS at $\alpha = 0.9$ $\rightarrow$ SNK at RNS pt CR to PW PW to CR	$\leftarrow$ PW to CR CR to PW $h_{max} \downarrow$	-	IB CR to PW	PW to CR CR to PW $\lambda_{max} \downarrow$ NS at $\lambda = 2.5$	NS Slow$\rightarrow$ PW to CR CR to PW	X	SNK at $q_z = 1.75$ PW to CR $q_{zc} \downarrow$
m	RNS at $\alpha = 0.9$ SNK at $\alpha = 0.9$ CR to PW PW to CR	$Pop_{max} \uparrow$ PW to CR	X	-	RNS $Pop_{max} \uparrow$ X	RNS $\downarrow$ $Pop_{max} \uparrow$ Satellites	RNS $\downarrow$ $Pop_{max} \uparrow$ X	$s_c \uparrow$ X
λ	RNS $\uparrow$ $Pop_{max} \uparrow$ SRC at $\alpha = 0.25$ PW to CR CR to PW	$Pop_{max} \uparrow$ $h_c \downarrow$ $\leftarrow$ CR to PW Satellites	$s_c \uparrow$ $Pop_{max} \uparrow$ PW to CR CR to PW	CR to PW $m_c \downarrow$ $Pop_{max} \uparrow$ PW to CR	-	$c_c \downarrow$ $\rightarrow$ SB to CR	RNS $q_{yc} \uparrow$ $Pop_{max} \uparrow$ Satellites	$q_{zc} \downarrow$ $\leftarrow$ CR to PW
c	SRC at RNS pt $\leftarrow$ MS satellites SNK at $\alpha = 0.3$	$Pop_{max} \uparrow$ PW to CR	$c_c \downarrow$ Quasi periodic SNK at $s = 0.5$	CB at $c = 1.8$ Bubble expands SB to CR Quasi periodic	$\lambda_c \downarrow$ Satellites PW to CR	-	RNS $\uparrow$ PW to CR	SRC at $q_z = 1.5$ PW to CR NS
q_y	RNS $\alpha = 0.9$ OD at $q_y = 1.42$ PW to CR before $q_y = 1.42$.	MS PW CR OD at $q_y = 1.35$	$s_c \uparrow$ OD at $q_y = 1.35$ PW CR CB CW	PW CR Satellites $\leftarrow$	SNK SB to CR PR to SB $\lambda_{max} \uparrow$	$\rightarrow$ OD at $q_y = 1.35$	…	$\leftarrow$ SB to CR CR to SB RNS $\downarrow$
q_z	RNS $\alpha = 0.9$ $\rightarrow \alpha_c \downarrow$	X	PW TO CR $Pop_{max} \uparrow$	$Pop_{max} \uparrow$ X	NS $\leftarrow$	$Pop_{max} \uparrow$ CR to PW	$Pop_{max} \uparrow$	…

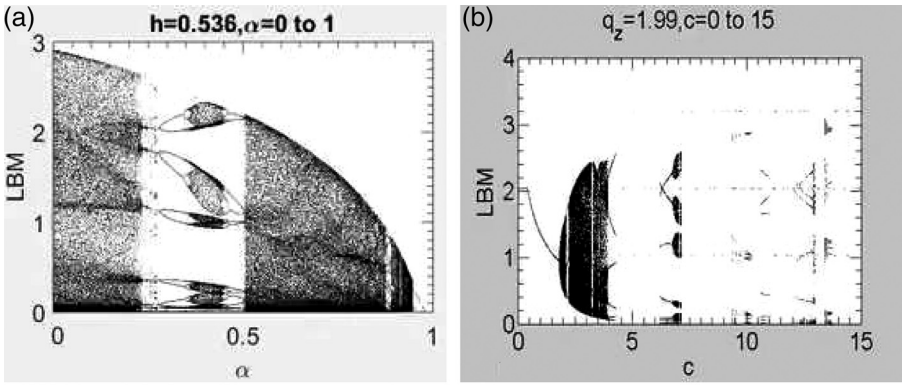

FIG. 16. Chaotic bubbles and multistability. (a) Screenshot of a bifurcation diagram video with respect to α for varying h showing chaotic bubbles for the 3-d system (one parasitoid species). Parameters: $\lambda = 8$, $q_y = 1.13$, $m = 13, c = 12, s = 0.5$, and $q_z = 1.34$ (Multimedia view). (b) Screenshot of a bifurcation diagram video with respect to c for varying q_z. At $c = 7$, seven stable limit cycles simultaneously exist. An interesting view of this is depicted in Fig. 13. Parameters: $\lambda = 8$, $q_y = 1.13$, $m = 13$, $h = 0.5$, $s = 0.5$, $\alpha = 0.5$. (Multimedia view) [URL: http://dx.doi.org/10.1063/1.4962633.3] [URL: http://dx.doi.org/10.1063/1.4962633.4]

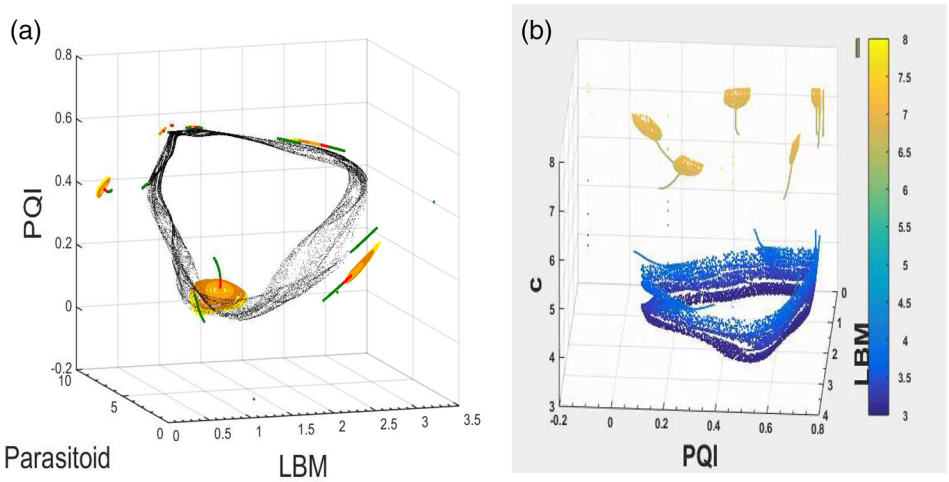

FIG. 17. Detail of the simultaneously existing 7 stable limit cycles of Fig. 16(b) seen from a different perspective. ($m = 13$, $\alpha = 0.5$, $h = 0.5$, $s = 0.5$, $q_y = 1.13$, $q_z = 1.99$). (a) Screenshot of the 3-d phase portrait of the system. (Multimedia view). (b) 2-dimensional bifurcation diagram for the variables x (LBM) and z (PQI) with respect to c (colour scale) showing the 7 (narrow) limit cycles of different sizes, having the appearance of dancing tulips. (Multimedia view) [URL: http://dx.doi.org/10.1063/1.4962633.5] [URL: http://dx.doi.org/10.1063/1.4962633.6]

behaviours, such as bursting, partial oscillation death, complete oscillation death, and co-existence of solutions in the dynamics of the larch budmoth. The system shows bursting behaviour for a certain parameter domain when two or more parasitoid species are present.

The parameters h and s introduced in our model track the changes in the environment due to global warming, use of pesticides, etc. Both terms regulate the dynamics and are required to correctly reproduce the relative frequencies of budmoth outbreaks as recorded in observational data.[7]

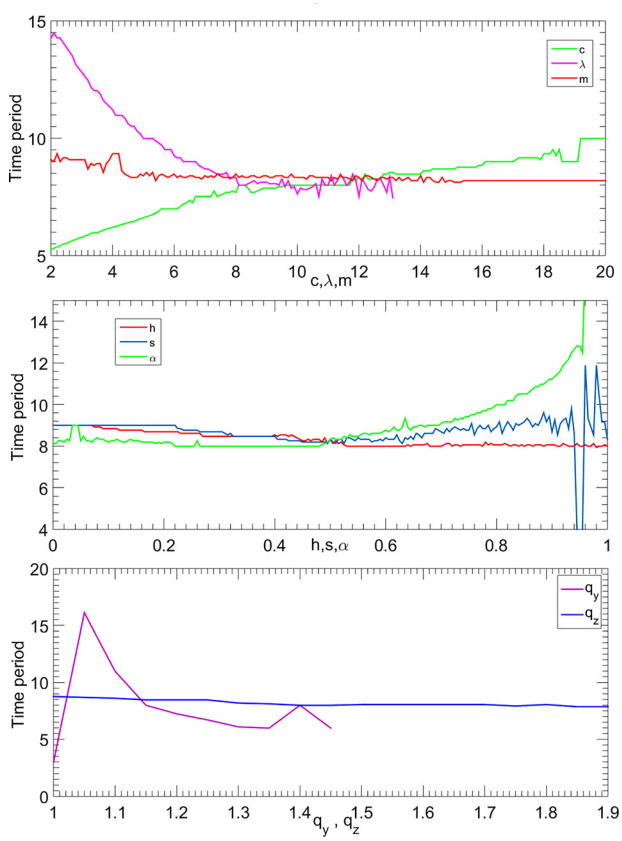

FIG. 18. Time period of cyclic outbreaks for the 3-d system (one parasitoid species) and its response with change in one parameter keeping other parameter values fixed at $\alpha = 0.5$, $h = 0.5$, $s = 0.5$, $\lambda = 8$, $q_y = 1.13$, $m = 13$, $c = 12, q_z = 1.34$.

The periodic cycles seen in this system are produced via a Neimark–Sacker bifurcation with respect to all parameters except q_y with respect to which there is a reverse Neimark–Sacker bifurcation wherein a limit cycle loses its stability and becomes a stable fixed point after becoming a stable spiral. Thus changes in parameter values due to perturbations can move the system to a regime which does not support the Neimark–Sacker bifurcation, the absence of periodic behaviour implying that there are no population cycles in the region being studied.

Observations made for over 50 years and the reconstructed data from tree rings studies[1] show a dominant 8 to 9 year periodicity in the budmoth outbreaks in the Engadine region of the Swiss Alps which our model reproduces. Our model with one parasitoid shows periodic variation of all the three interacting species, which are mutually synchronized with a small constant phase lag, in accordance with observations. The bifurcation videos for the 3-species system, some of which we have made available in the supplementary multimedia files, show remarkable dynamics the system can generate. Some of the notable features are the creation and annihilation of fixed points at certain value of parameters, creation of chaotic regions via bubble formation, expansion or contraction of the attractor size via interior crises, and creation of satellites due to interior crises. The presence of bubbles, including chaotic bubbles indicates that the hydra effect, involving an increase in the population size of a species in response to an increased mortality rate—an important feature in population dynamics is prevalent in our model. This in turn indicates that several routes exist in our complex tritrophic system by which extinction of any of the species may be avoided.

Our model is also more robust than earlier models in the literature. Further our model can not only explain the observed collapse of the budmoth cyclic outbreaks in the Swiss Alps after 1981 but also account for the historical absence of cycles in the nearby Tatra mountains in the Carpathians.[7] Our system with four or more species produces cycles too. However the introduction of one or more parasitoid species to the 3-dimensional system causes the time periods of budmoth outbreak cycles to become longer. The simultaneous presence of more than one parasitoid in our

model mimics a realistic situation because in nature the budmoth may be parasitized by 94 species of parasitoids.[24] Indeed, observations have recorded the presence of as many as 5.4 species of parasitoids on the average on a single budmoth in the Swiss Alps in a year.[25] Such a possibility of the presence of more than one parasitoid species in the budmoth system has, to our knowledge, never been studied before in a mathematical model in the literature.

ACKNOWLEDGMENTS

S.V.I. thanks CSIR (Center for Scientific and Industrial Research) New Delhi, India, for funding.

APPENDIX: LINEAR STABILITY ANALYSIS AND CONCLUSIONS FROM THE ROUTH ARRAY

The Jacobian of the system evaluated at the fixed points (x^*, y^*, v^*, z^*) is given by the matrix: $\begin{pmatrix} A & B & C & D \\ E & F & G & H \\ I & J & K & L \\ M & N & O & P \end{pmatrix}$

whose entries are given by

$$A = \frac{\lambda\rho_z z^*}{1+\mu_z^* z^*}(1-x^*)\exp\left(-x^* - \frac{\rho_y y^*}{1+\mu_y y^*} - \frac{\rho_v v^*}{1+\mu_v v^*}\right)$$

$$B = -\frac{\lambda\rho_z z^* x^*}{1+\mu_z z^*}\frac{\rho_y}{(1+\mu_y y^*)^2} \times \exp\left(-x^* - \frac{\rho_y y^*}{1+\mu_y y^*} - \frac{\rho_v v^*}{1+\mu_v v^*}\right), \quad \text{(A1)}$$

$$C = -\frac{\lambda\rho_z z^* x^*}{1+\mu_z z^*}\frac{\rho_v}{(1+\mu_v v^*)^2} \times \exp\left(-x^* - \frac{\rho_y y^*}{1+\mu_y y^*} - \frac{\rho_v v^*}{1+\mu_v v^*}\right)$$

$$D = \lambda x^* \frac{\rho_z}{(1+\mu_z z^*)^2}\exp\left(-x^* - \frac{\rho_y y^*}{1+\mu_y y^*} - \frac{\rho_v v^*}{1+\mu_v v^*}\right)$$

$$E = c\left(1 - \exp\left(-\frac{\rho_y y^*}{1+\mu_y y^*}\right)\right)$$

$$F = cx^*\frac{\rho_y}{(1+\mu_y y^*)^2}\exp\left(-\frac{\rho_y y^*}{1+\mu_y y^*}\right)$$

$$G = 0; \quad H = 0$$

$$I = \kappa c\left(1 - \exp\left(-\frac{\rho_v v^*}{1+\mu_v v^*}\right)\right); \quad J = 0$$

$$K = \kappa c x^* \frac{\rho_v}{(1+\mu_v v^*)^2}\exp\left(-\frac{\rho_v v^*}{1+\mu_v v^*}\right); \quad L = 0$$

$$M = -\left(\frac{(1-\alpha)m}{(m+x^*)^2} + \alpha s\frac{\rho_z z^*}{1+\mu_z z^*}\right)$$

$$N = 0; \quad O = 0; \quad P = \frac{\alpha(h-sx^*)\rho_z}{(1+\mu_z z^*)^2}. \quad \text{(A2)}$$

Its characteristic equation is given by

$$c_1\Lambda^4 + c_2\Lambda^3 + c_3\Lambda^2 + c_4\Lambda + c_5 = 0,$$

TABLE IV. Routh–Hurwitz criterion: $h = 0.5$, $s = 0.5$, $\alpha = 0.5$, $m = 13$, $c = 12$, $q_y = 1.13$, $q_z = 1.34$, and $q_v = 1.13$.

Fixed points (x^*, y^*, v^*, z^*)	RH-coeff	Stability	λ κ
0, 0, 0, 0.6936	All positive	Stable	$\lambda = 1$
0.01, 0.001, 0, 0.6936	One negative	Unstable	$\lambda = 8, \kappa = 0.3$
0.01, 0, 0.001, 0.6936	One negative	Unstable	$\lambda = 8, \kappa = 1.8$
0.001, 0.2, 0.1, 0.6936	One negative	Unstable	$\lambda = 8, \kappa = 1.08$
0.001, 0.2, 0.1, 0.6936	One negative	Unstable	$\lambda = 9, \kappa = 1.08$
0.001, 0.2, 0.1, 0.6936	One negative	Unstable	$\lambda = 5, \kappa = 1.2$
0.001, 0.2, 0.1, 0.6936	One negative	Unstable	$\lambda = 8, \kappa = 0.9$
0.001, 0.2, 0.1, 0.6936	One negative	Unstable	$\lambda = 7, \kappa = 1.3$
0.5, 0.2, 0.1, 0.6936	One negative	Unstable	$\lambda = 8, \kappa = 1.0$

where

$$c_1 = 1; \quad c_2 = -(A+F+K+P)$$

$$c_3 = AF - BE + AK - CI + AP - DM + FK + FP + KP$$

$$c_4 = BEK - AFK + CFI - AFP + BEP + DFM - AKP + CIP + DKM - FKP$$

$$c_5 = AFKP - BEKP - CFIP - DFKM.$$

The Routh array constructed from the Jacobian matrix is:

$$\begin{pmatrix} c_1 & c_3 & c_5 \\ c_2 & c_4 & 0 \\ \frac{c_2c_3 - c_1c_4}{c_2} & c_5 & 0 \\ \frac{-(c_5c_2^2 - c_3c_2c_4 + c_1c_4^2)}{(c_2c_3 - c_1c_4)} & 0 & 0 \\ c_5 & 0 & 0 \end{pmatrix}$$

Since the system poses difficulty in solving analytically, we resort to numerical methods to find its stability. Some of these numerical results are shown in Table IV.

The condition $c_4(c_2c_3 - c_4) - c_5c_2^2 = 0$ ensures formation of a limit cycle[43,44] and appearance of a pair of imaginary eigenvalues. The frequency ω of this limit cycle is given by $\omega^2 = \frac{c_4}{c_2}$.

For $\lambda = 1$, limit cycles do not form; the Routh–Hurwitz (RH) coefficients are all positive indicating that it is a stable fixed point. As we vary λ to 8, the fixed point loses its stability, becoming an unstable spiral with a limit cycle being born around it. For $\lambda = 8$ one of the RH coefficients is negative which indicates the fixed point losing its stability. Similarly, we see that when one of the parasitoids does not exist (3-d system), RH coefficients of different signs arise for large values of λ.

[1]J. Esper, U. Büntgen, D. C. Frank, D. Nievergelt, and A. Liebhold, "1200 years of regular outbreaks in alpine insects," Proc. R. Soc. London, Ser. B **274**, 671–679 (2007).
[2]O. Konter, J. Esper, A. Liebhold, T. Kyncl, L. Schneider, E. Düthorn, and U. Büntgen, "Tree-ring evidence for the historical absence of cyclic larch budmoth outbreaks in the Tatra Mountains," Trends. Ecol. Evol. **29**, 809–814 (2015).

[3]W. Baltensweiler and A. Fischlin, "The larch budmoth in the Alps," in *Dynamics of Forest Insect Populations* (Springer, New York, 1988), pp. 331–351.
[4]W. Baltensweiler, "Why the larch bud-moth cycle collapsed in the subalpine larch-cembran pine forests in the year 1990 for the first time since 1850," Oecologia **94**, 62–66 (1993).
[5]A. A. Berryman, "What causes population cycles of forest Lepidoptera?," Trends. Ecol. Evol. **11**, 28–32 (1996).
[6]G. Battipaglia *et al*., "Long-term effects of climate and land-use change on larch budmoth outbreaks in the French Alps," Clim. Res. **62**, 1–14 (2014).
[7]S. V. Iyengar, J. Balakrishnan, and J. Kurths, "Impact of climate change on larch budmoth cyclic outbreaks," Sci. Rep. **6**, 27845 (2016).
[8]L. Euler, *Introduction in Analysis Infinitorum* (Bousquet, Lausanne, 1748).
[9]E. Heine, *Handbuch der Kugelfunktionen* (Reimer, Berlin, 1878), Vol. 1, reprinted by Physica-Verlag, Wurzburg (1961).
[10]F. H. Jackson, "A generalization of the functions $\Gamma(n)$ and x^n," Proc. R. Soc. London **74**, 64–72 (1904).
[11]F. H. Jackson, "On q-functions and a certain difference operator," Trans. - R. Soc. Edinburgh **46**, 253–281 (1909).
[12]T. Geisel and S. Thomae, "Anomalous diffusion in intermittent chaotic systems," Phys. Rev. Lett. **52**, 1936 (1984).
[13]C. Tsallis, "Possible generalization of Boltzmann-Gibbs statistics," J. Stat. Phys. **52**, 479–487 (1988).
[14]C. Beck, E. G. D. Cohen, and S. Rizzo, "Atmospheric turbulence and superstatistics," Europhys. News **36**, 189–191 (2005).
[15]S. Abe, U. Tirnakli, and P. A. Varotsos, "Complexity of seismicity and nonextensive statistics," Europhys. News **36**, 206–208 (2005).
[16]A. R. Plastino and A. Plastino, "Stellar polytropes and Tsallis' entropy," Phys. Lett. A **174**, 384–386 (1993).
[17]A. Rapisarda and A. Pluchino, "Nonextensive thermodynamics and glassy behaviour," Europhys. News **36**, 202–206 (2005).
[18]G. Kaniadakis, A. Lavagno, and P. Quarati, "Generalized statistics and solar neutrinos," Phys. Lett. B **369**, 308–312 (1996).
[19]E. Lutz, "Anomalous diffusion and Tsallis statistics in an optical lattice," Phys. Rev. A **67**, 051402(R) (2003).
[20]P. Douglas, S. Bergamini, and F. Renzoni, "Tunable tsallis distributions in dissipative optical lattices," Phys. Rev. Lett. **96**, 110601 (2006).
[21]P. Turchin, *Complex Population Dynamics: A Theoretical/Empirical Synthesis* (Princeton University Press, NJ, 2003).
[22]P. Turchin *et al*., "Dynamical effects of plant quality and parasitism on population cycles of larch budmoth," Ecology **84**, 1207–1214 (2003).
[23]P. Turchin *et al*., "Population cycles of the larch budmoth in Switzerland," in *Population cycles: The case of trophic interactions*, edited by A. Berryman (Oxford University Press, 2002), pp.130–141.
[24]V. Delucchi, "Parasitoids and hyperparasitoids of Zeiraphera Diniana and their role in population control in outbreak areas," Entomophaga **27**, 77–92 (1982).
[25]N. J. Mills, "Observations on the parasitoid complexes of budmoths (Lepidoptera: Tortricoidea) on larch in Europe," Bull. Entomol. Res. **83**, 103–112 (1993).
[26]W. E. Ricker, "Stock and recruitment," J. Fish. Res. Board Can. **11**, 559–623 (1954).
[27]A. J. Nicholson and V. A. Bailey, "The balance of animal populations, Part I," J. Zool. **105**, 551–598 (1935).
[28]C. S. Holling, "Some characteristics of simple types of predation and parasitism," Can. Entomol. **91**, 385–398 (1959).
[29]S. R.-J. Jang and D. M. Johnson, "Dynamics of discrete-time larch budmoth population models," J. Biol. Dyn. **3**, 209–223 (2009).
[30]J. R. Beddington, "Mutual interference between parasites or predators and its effect on searching efficiency," J. Anim. Ecol. **44**, 331–340 (1975).
[31]A. J. Lotka, "Undamped oscillations derived from the law of mass action," J. Am. Chem. Soc. **42**, 1595–1599 (1920).
[32]A. J. Lotka, *Elements of Physical Biology* (Williams and Wilkins, Baltimore, 1925).
[33]V. Volterra, "Variazionie fluttuazioni del numero d'individui in specie animali conviventi," Mem. R. Accad. Naz. dei Lincei **2**, 31–113 (1926); V. Volterra, "Variations and fluctuations of the numbers of individuals in animal species living together," Translation by R. N. Chapman, in *Animal Ecology* (McGraw-Hill, New York, 1931), pp. 409–448.
[34]P. C. Reid *et al*., "Global impacts of the 1980 regime shift," Glob. Chang. Biol. **22**, 682–703 (2016).
[35]E. Brocard *et al*., "Upper air temperature trends above Switzerland 1959–2011," J. Geophys. Res. Atmos. **118**, 4303–4317 (2013).
[36]A. J. Allstadt, K. J. Haynes, A. M. Liebhold, and D. M. Johnson, "Long-term shifts in the cyclicity of outbreaks of a forest-defoliating insect," Oecologia **172**, 141–151 (2013).
[37]D. M. Johnson *et al*., "Climatic warming disrupts recurrent Alpine insect outbreaks," Proc. Natl. Acad. Sci. U.S.A. **107**, 20576–20581 (2010).
[38]N. Gilbert, "What they didn't tell you about limit cycles," Oecologia **65**, 112–113 (1984).
[39]S. V. Iyengar and J. Balakrishnan, "q-deformations and the dynamics of the larch bud-moth population cycles," in *Nature's longest threads: New Frontiers in the Mathematics and Physics of Information in Biology*, edited by J. Balakrishnan and B. V. Sreekantan (World Scientific Publishing Company Pte. Ltd., Singapore, 2014), Chap. 8, pp. 65–80.
[40]A. Koseka, E. Volkov, and J. Kurths, "Oscillation quenching mechanisms: Amplitude vs. oscillation death," Phys. Rep. **531**, 173–199 (2013).
[41]P. A. Abrams, "When does greater mortality increase population size? The long history and diverse mechanisms underlying the hydra effect," Ecol. Lett. **12**, 462–474 (2009).
[42]C. N. K. Anderson *et al*., "Why fishing magnifies fluctuations in fish abundance," Nature **452**, 835–839 (2008).
[43]J. Guckenheimer and P. Holmes, *Nonlinear Oscillations, Dynamical Systems, and Bifurcations of Vector Fields* (Springer Verlag, 1983), Vol. 42.
[44]M. Han and P. Yu, *Normal Forms, Melnikov Functions and Bifurcations of Limit Cycles* (Springer Verlag, 2012), Vol. 181.